

# GeV Gamma-ray Counterparts of New Candidate Radio Supernova Remnants Detected in the GLEAM Survey

B.M. Meşe<sup>1</sup>, T.Ergin<sup>2</sup>

<sup>1</sup> Middle East Technical University, Department of Physics, ODTU Campus, 06800, Ankara, Turkey; mina.mese@metu.edu.tr <sup>2</sup> Middle East Technical University, Northern Cyprus Campus, 99738 Kalkanli via Mersin 10, Turkey; ergin.tulun@gmail.com

Recently the Galactic and Extra-galactic All-sky Murchison Widefield Array survey has published 27 new candidate radio supernova remnants (SNRs) which are located within the longitude ranges of  $345^\circ < l < 60^\circ$  and  $180^\circ < l < 240^\circ$ . To search for the gamma-ray counterparts of these candidate radio SNRs, we analyzed 14 years of Fermi-LAT data in the energy range of 0.2–300 GeV. There are three promising SNRs; G18.9-1.2, G23.1+0.1, and G28.3+0.2, which we detected at a significance level of  $11\sigma$ ,  $6.1\sigma$ , and  $20.6\sigma$ , respectively. Here we report the results of our morphological and spectral analyses of G18.9-1.2, G23.1+0.1, and G28.3+0.2.

## Introduction

There are three promising sources: G18.9-1.2, G23.1+0.1, and G28.3+0.2. G23.1+0.1 is detected with a test statistics (TS) value of 37.41, and it is associated with HESS J1832-085, which is an unidentified VHE gamma-ray source. It is a point-like source, best modeled with the power law model. It is associated with the pulsar PSR J1832-0836 [2]. It has a shell-type radio morphology and radio spectral index (RSI) value of  $-0.64 \pm 0.05$ . The 200-MHz flux density is  $17.3 \pm 0.4$ . 4FGL J1832.4-0847 source lies inside the error ellipse of the GLEAM source, but it is not associated and this GLEAM source is not detected by the 4FGL catalog. Its age is about  $10^4$  yr and its distance is  $\sim 4.6$  kpc [4,5].

G18.9-1.2 is a shell-type SNR and associated with the SNR G018.9-01.1, and it coincides with the 4FGL J1829.4-1256 source. It is detected by the Fermi telescope and named 3FGL J1829.7-1304, but it is not detected by the 4<sup>th</sup> Fermi catalog. It has a significance of  $9.5\sigma$ . It contains a pulsar wind nebula and pulsar candidate named CXOU J182913.1-125113. The SNR's age is  $\sim 2800$ – $6100$  yr and its distance is  $\sim 1.6$ – $2.5$  kpc. It is also detected by ROSAT, Chandra, and ASCA.

G28.3+0.2 is a shell-type SNR with  $13.7\sigma$  significance. It coincides with the 4FGL J1842.5-0359 source; and it is located near NVSS J184240-035858, which is an extra-galactic radio source. It has a possible PSR association but it is not certain, therefore the SNR's age and distance are not determined.

| Name      | RA / DEC          | Association       |
|-----------|-------------------|-------------------|
| G18.9-1.2 | 277.517 / -13.000 | 4FGL J1823-1256   |
| G23.1+0.1 | 278.179 / -8.633  | 4FGL J1832.4-0847 |
| G28.3+0.2 | 280.592 / -3.967  | 4FGL J1842.5-0359 |

Table 1. Right ascension (RA) and declination (DEC) values of the GLEAM sources in degrees, and the associations with 4<sup>th</sup> Fermi catalog (4FGL) objects are shown.

## Methods

For the analysis, we use  $\sim 14$  years of gamma-ray data of Fermi Large Area Telescope (Fermi-LAT), FermiTools v1.2.23, and FermiPy v0.17.4 analysis packages provided by NASA. We have used Python v2.7.14 and ipython v5.8.0.

1) FermiTools is used for data reduction, which consists of event selection and time selection. Event selection is made with *gtselect*, by mainly cutting the time, energy, position, and maximum zenith angle. For the time selection purpose, *gtmktime* is used to cut the spacecraft parameters and update the good time interval (GTI). Binned likelihood analysis is chosen and using the latest background and diffuse models which are galactic interstellar emission model v7 and isotropic template v2.1, an XML file is created. To perform the likelihood analysis faster, live-times and exposure are pre-computed and the live-time is applied to the regions of interest (ROI). Finally, the data set is ready for running *glike* to complete the likelihood analysis. The energy interval is chosen as 0.2-300 GeV.

2) *Sky Map Production and Study of the SNR Structure (Morphology)* The locations of the sources are obtained from the GLEAM data. The major and minor axes in arcminutes, and the position angle CCW from the north of the ellipses are 68, 60, 355 for G18.9-1.2; 26, 26, 0 for G23.1+0.1; and 14, 14, 0 for G28.3+0.2, respectively. Two TS maps are created at the 1-300 GeV energy range for each source: before and after a best-fitting location is used and a best-fitting extension model is applied. The best locations are found by deleting the associated 4FGL sources from the background models and running the *localize()* script. Then, the sources are re-added at these locations with the original spectral models of each source used at the models, which are log parabola (LP) for G18.9-1.2 and G28.3+0.2, and power law (PL) for G23.1+0.1. To model the extensions of the target objects, the *extension()* method, which contains two 2-D models; radial disk (RD) and radial gaussian (RG) is used. The results with largest TS-ext values are selected as the best-fitting models for each source. After these models are applied, a second TS map is created for each source and displayed by the image display tool DS9. Spectral energy distribution (SED) Graphs at the energy range of 0.2–300 GeV is created for the associated 4FGL sources.

## References

- [1] Hurley-Walker, Natasha, et al. *Publications of the Astronomical Society of Australia* 36 (2019)
- [2] Abdalla, H., et al. *Astronomy & Astrophysics* 612 (2018): A1.
- [3] Condon, James J., et al. *The Astronomical Journal* 115.5 (1998): 1693
- [4] Maxted, Nigel I., et al. *The Astrophysical Journal* 885.2 (2019): 129
- [5] Ergin, Tulun, and Şen, Ayşegül, 43rd COSPAR Scientific Assembly. Held 28 January-4 February 43 (2021): 1490
- [6] Abdollahi, Soheila, et al. *The Astrophysical Journal Supplement Series* 247.1 (2020): 33
- [7] <https://fermipy.readthedocs.io/en/latest/>
- [8] <https://fermi.gsfc.nasa.gov/ssc/data/analysis/documentation/Cicerone/>

| Analysis & Results |        |        |                           |                          |                           |
|--------------------|--------|--------|---------------------------|--------------------------|---------------------------|
| Name               | TS     | TS-ext | Alpha                     | Beta                     | Norm                      |
| G18.9-1.2          | 104.91 | 1.527  | $2.946 \pm 0.2511$        | $0.5756 \pm 0.2511$      | $4.493e-13 \pm 7.275e-14$ |
| G28.3+0.2          | 423.96 | 13.718 | $3.157 \pm 0.3754$        | $0.6248 \pm 0.1717$      | $2.12e-12 \pm 3.782e-13$  |
| Name               | TS     | TS-ext | Prefactor                 | Index                    | Scale                     |
| G23.1+0.1          | 204.89 | 8.345  | $8.962e-12 \pm 6.951e-13$ | $-0.2641 \pm \text{nan}$ | $3068 \pm \text{nan}$     |

Table 2. Test statistics (TS) and extension TS (TS-ext) values at 1-300 GeV energy range for the best fitting models are shown. Upper panel: LP+RD model for G18.9-1.2, and LP+RD model for G28.3+0.2 are used. Lower panel: PL+RD model for G23.1+0.1 is used.

We made spectral and extension model tests for all three objects at the 1-300 GeV energy range when the associated 4FGL sources are deleted from the background models. The best-fitting models are determined as LP+RD for G18.9-1.2, PL+RD for G23.1+0.1, and LP+RD for G28.3+0.2. TS maps are created in the 1–300 GeV energy range. The TS maps shown on the left in Figure 2 are produced before the best fitting extension model is applied. The TS maps on the right are produced after the associated 4FGL objects are deleted from the background model and re-added at the best-fitting location with the best-fitting extension model, with the original spectral model. Figure 1 shows the associated 4FGL sources' SED graphs at 0.2–300 GeV energy range.

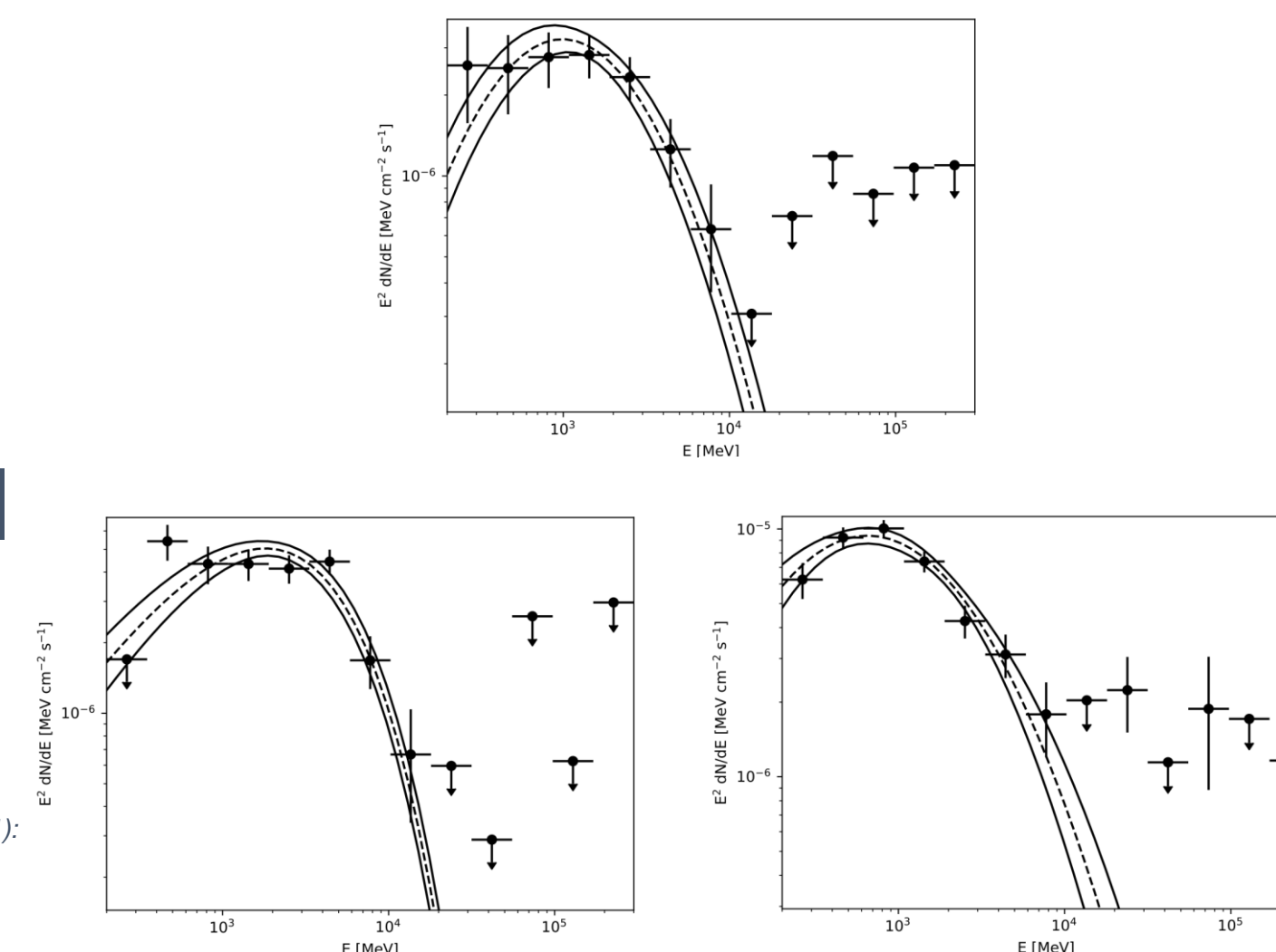


Figure 1. Spectral energy distribution (SED) graphs of the associated 4FGL sources at 0.2–300 GeV. The x-axis shows the energy in MeV and the y-axis is  $E^2 dN/dE$  in the unit of  $\text{MeV cm}^{-2} \text{s}^{-1}$ . Upper panel: G18.9-1.2, Lower left panel: G23.1+0.1, Lower right panel: G28.3+0.2.

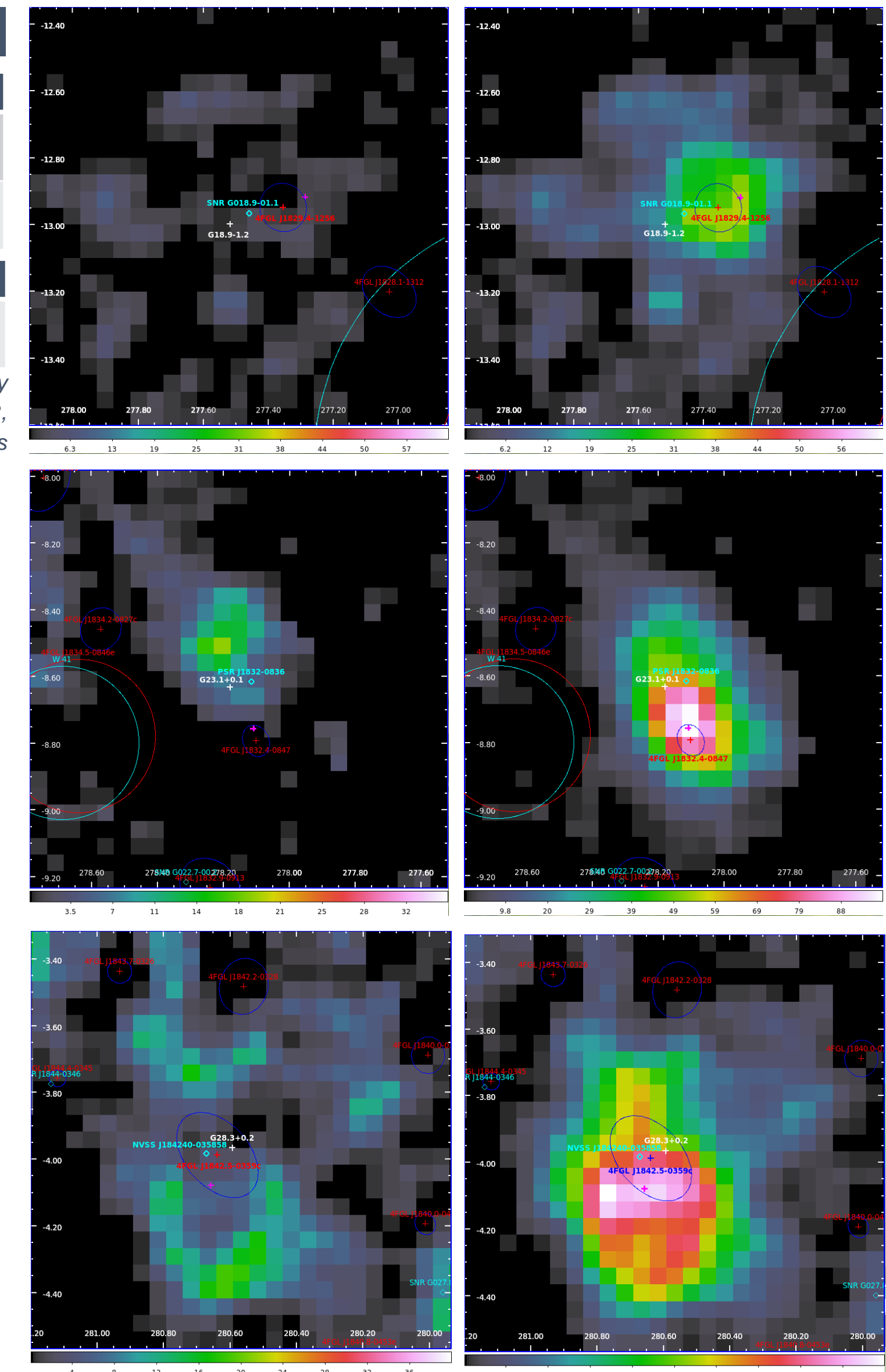


Figure 2. TS maps at 1–300 GeV energy range. The RA-DEC values in degrees are shown at the x-y axes. The cyan diamonds represent the associated sources. 4FGL sources are shown with red crosses and the blue ellipses are the error ellipses of them. The GLEAM positions are shown with white crosses. The best locations detected are shown as magenta crosses. Upper panel: G18.9-1.2, before (left) and after (right) the LP+RD model is applied. Middle panel: before (left) and after (right) the PL+RD model is applied. Lower panel: G28.3+0.2, before (left) and after (right) the LP+RD model is applied. The associated 4FGL source is shown with a blue cross on the right-hand side TS map.